SEISMIC ANALYSIS OF THE INTERSTATE 5 AND HIGHWAY 14 CONNECTOR BRIDGE

Robert K. Dowell

Dowell-Holombo Engineering, Inc.
San Diego, California

Abstract

As part of the Strong-Motion Instrumentation Program in California (CSMIP), several bridge structures have been instrumented to record accelerations for the duration of each earthquake event that strikes. The subject of this paper is the investigation of the measured and calculated responses of the heavily instrumented 10-span connector bridge (53-2795F) at the 5/14 Interchange, subjected to a recorded earthquake. A detailed computer model of the bridge structure was developed, allowing comparisons to measured response quantities for many of the 42 sensor locations. In order to compare measured and computed results it was necessary to develop global axes that were common to both the bridge model and structure instrumentation.

Introduction

In order to better understand seismic bridge behavior of a real structure subjected to an actual earthquake, the 10-span connector bridge (53-2795F) at the 5/14 Interchange has been instrumented with 42 channels of data acquisition, measuring accelerations at different locations along the bridge superstructure as well as at the abutments and base of several columns. By integrating recorded accelerations, the velocity and displacement time-history responses are also determined. The recording devices are automatically triggered by small accelerations at the beginning of an earthquake and thus the complete earthquake history is recorded at 0.01 second time intervals at all sensor locations. Of the three earthquakes listed on the CSMIP site for the Sylmar 5/14 Interchange, only the Magnitude 7.1 Hector Mine Earthquake is discussed here, as it produced approximately 50 times more displacement than the other 2 earthquakes. The Hector Mine Earthquake occurred on October 16, 1999 with the epicenter 47 miles ESE of Barstow.

The overall bridge structure and locations of strong-motion instrumentation are shown in Figure 1. It is a cast-in-place, prestressed, concrete box girder bridge with 10 spans supported by single column bents and pile shafts. There is one expansion joint hinge in the bridge superstructure, placed between Bents 5 and 6. Rather than the hinge being at about the 20% span location, as is typically done in bridge design, the hinge is right in the middle of the span. This is because Span 5 is a very short 26 ft, with 13 ft cantilevers on either side of the hinge. Such a design concept was chosen so that collapse could no occur from unseating of the long span at the hinge, as had occurred to the previous bridge at this site. Thus the connector bridge consists of two separate bridge frames from Abutment 1 to the expansion joint hinge in Span 5 and from this hinge to Abutment 11. The abutments are seat-type, indicating that they are not integral with the bridge superstructure. In order to have similar stiffness' at all bents, column isolation casings are

provided at some of the bents, which increase the effective length of the columns below the ground line.

Measured results from the Magnitude 7.1 Hector Mine earthquake are provided in this paper. Also, a discussion of the computer model is given and some comparisons to the measured results are shown. Difficulties in determining the input motions to be used in the model are discussed, as well as how to model the soil at the foundations. Nonlinear and linear time-history analyses as well as modal versus direct time-step integration methods are discussed. It should be noted that development of the detailed structural model is currently underway and that the paper discusses the current state of the modeling as well as modifications that will be made to the model in the near future as part of the ongoing Lifeline Structure Response Project.

Measured Results from Strong-Motion Instrumentation

Loading at the Base of the Structure

This section presents various results that were measured on or near the bridge of interest from the Hector Mine Earthquake discussed above. In order to compute relative motions between the bridge superstructure and the base input, it is important to understand the overall loading of the bridge and to determine if the abutments and columns were being loaded with different ground motions or essentially the same motion. At first glance, the local longitudinal and transverse displacement time-history responses of Abutments 1 and 11 indicate that they are, indeed, being subjected to different ground motions (Figures 2 and 3), possibly due to the distance between abutments and the variations in soil type and depth. Note that in these figures C2 and C35 are the channel designations for local longitudinal responses at Abutments 1 and 11, respectively. Channels C1 and C33 represent local transverse instrumentation at Abutments 1 and 11, respectively. Throughout the paper the term “local” refers to the instrument direction indicated in Figure 1. Along the bridge superstructure and at the abutments this local direction is tangent to the bridge alignment. At the base of the columns and at the freefield instrumentation, the local alignment of the channels is north, as shown in Figure 1.

Since measured displacement time-history results at the two abutments, presented in Figures 2 and 3, are given in local coordinates it is not clear if they appear so different from one another due to the varied orientations of the instruments, or if there is a real difference in the ground motions at either end of the bridge. One way to compare the results is to determine the absolute displacement at each point in time for both abutments and plot them on top of each other for the duration of the earthquake. To obtain the absolute displacement requires that the two orthogonal results in plan view be recorded, allowing the square root of the sum of the square of the two orthogonal components to be found for each time interval. The results shown in Figure 4 clearly demonstrate that total displacements at the two abutments and column base of Bent 5 are very similar for the full 80 seconds duration of ground shaking. Note that total displacement is always positive as it represents the distance in plan view from the origin to the displaced location, giving an instantaneous radius. While this result is encouraging, it does not guarantee that the ground motions are the same along the bridge structure, as the angle of the total displacements could be different. For example, at a given point in time the total displacement might be the same at the two abutments but the movement could be in a completely

different direction, resulting in different longitudinal and transverse components. It is, however, very unlikely that the correlation would be as good as shown in Figure 4 for the full 80 seconds of loading unless the angle of displacement also matched closely.

Global responses are compared at the two abutments by converting the displacement time-history traces of the orthogonal channels into global longitudinal and global transverse directions. In keeping with standard seismic bridge design practice, a line connecting the centerline of the superstructure and the centerline of abutments in plan view is the global longitudinal axis of loading, which is rotated only 1.54 degrees from the north direction indicated in Figure 1, and the global transverse direction of loading is rotated 90 degrees from the global longitudinal axis. These global directions are used to view the measured data and to define the loading directions and input ground motions for the computer model. For each time increment the total displacement is found, as shown in Figure 4, and the angle of rotation is also found in relation to the global axes just defined. When the abutment motions are converted to global axes it is seen that both longitudinal and transverse time-history responses are very similar between the two abutments (Figures 5 and 6). Although not given in these figures, it was determined that the base of Bents 5 and 7 also followed the global abutment displacements very closely. Note that the notation that is now given in the figures shows that global longitudinal and transverse displacements are found from both orthogonal channels at a given location. For example, the legend "Longitudinal C1-2" indicates that local longitudinal and transverse motions from Channels C1 and C2 at Abutment 1 were used to determine the global longitudinal response. The same is required for global transverse displacements.

It is of interest to plot local transverse versus longitudinal displacements, as given in Figure 7. The distance from the origin to any point on the line represents the total displacement. It can be imagined that this graph is a view of the structure motion from above, in plan view, tracing longitudinal and transverse movements of Abutment 1, and sweeping out the curve given in Figure 7. Of course, in order to compare Abutment 1 and 11 responses on this type of plot the results must be rotated into global coordinates (see Figure 8). This figure shows that the abutment responses are very similar, as indicated previously, and yet they are not exactly the same, with varying amounts of transverse and longitudinal displacements. A line that borders the graph in Figure 8 represents an envelope of maximum displacements.

Joint Openings at Abutments and the Expansion Joint Hinge

Joint motions are given on both sides of each joint in local longitudinal and transverse coordinates at Abutments 1 and 11 and at the expansion joint hinge (Figures 9 through 14). What is clear from these figures is that at both abutments the transverse and longitudinal displacements are very similar on either side of the joint. However, at the expansion joint hinge the two responses on either side of the hinge are vibrating back and forth about each other, indicating relative movement between frames in both longitudinal and transverse directions (Figures 11 and 12). This is somewhat masked because the relative motion between frames is much smaller than the displacement of each frame. Note that the displacement includes the ground motion that the columns and abutments are subjected to.

Relative displacements between frames at the expansion joint hinge were calculated in the longitudinal and transverse directions by taking the difference in the measured displacements on either side of the hinge. The results are presented in Figures 15 and 16, showing a maximum relative transverse displacement of about 0.7 cm and a maximum relative longitudinal displacement of over 1 cm. These figures provide a much clearer picture of the behavior of the two frames at the hinge, showing that they move relatively freely from each other since the expansion joint is at the center of the span and a gap of at least 2 inches is provided between frames to allow for thermal movement. This structure is unusual in that the hinge is at the center of the span and neither span rests on the other, as is typically the case.

Relative Displacements between the Superstructure and Ground Input Motion

Of particular interest is the relative motion between the bridge superstructure and the base input motion or ground motion. This is a little difficult to define because the measured base motion is not identical at all locations along the structure alignment and this information is not available at all of the bents. However, to be consistent throughout the project it is important to clearly define the base motion of the bridge so that it can be subtracted from all other displacements for comparison purposes. This is also important for the structural modeling, as base input accelerations are required to load the model with the measured earthquake. Also, the relative motion from the model between the bridge superstructure and ground will depend on how the base motion is defined, and it must be consistent to have fair comparisons between measured and calculated results. It should be appreciated that to find relative motions requires subtracting large numbers from other large numbers, resulting in increased errors associated with instrument sensitivity and unwanted noise in the data.

As presented earlier, measured global longitudinal and transverse displacement time-histories at the abutments and at the column bases are very similar to each other and thus it was decided to define Channels C1 and C2 at Abutment 1 as the base motion for all future comparisons and analyses. This completely defines the input motion for the structural model. Note that at this point the vertical motions have not been included in the model. As discussed previously, the model is loaded along global longitudinal and transverse directions with base accelerations determined from Channels C1 and C2 at Abutment 1. Measured relative motions of the bridge superstructure at Bents 5, 6 and 7 are given in Figures 17 through 22 for both transverse and longitudinal directions. Also provided in these figures are results from preliminary time-history analyses of the bridge model. Details of the computer model are discussed in the next section. The analysis results are quite good in the global transverse direction at Bent 5 for the duration of loading, with approximately 1.5 cm of maximum relative displacement between the deck and ground (Figure 18). However, in the global longitudinal direction at Bent 5 the model over-predicts maximum measured displacements by about 50 percent (Figure 17). Maximum calculated relative deck displacements at Bents 6 and 7 are similar to maximum measured response, but the time-history traces do not follow the measured results as closely as in the transverse direction for Bent 5. The maximum measured relative response in the longitudinal direction is about 0.7 cm, while in the transverse direction it is approximately 1.7 cm. Note that measured freefield motion was found to vary significantly from measured abutment and column base motions, and was therefore not used in the present analysis. Clearly this will need to be further investigated.

Computer Model

A computer model was developed for the connector structure (Figure 23) using SAP2000, Version 8 [1]. The bridge superstructure, columns and pile shafts were all modeled with beam elements. Four beam elements were used per span and three beam elements were used per column. Large diameter pile shafts were modeled with nodes spaced at five feet to accommodate longitudinal and transverse soil springs to the model. Initially it was thought that cyclic nonlinear soil springs were needed along the height of the pile shafts. However, measured results from the earthquake have demonstrated that the ground deformations are small enough to assume liner-elastic soil springs. The stiffness' of the longitudinal and transverse soil springs are based on the initial stiffness given in [2] for the soils listed in the log of test borings. Member geometry follows the centroid of the members in 3-D space. Stiffness values were provided in the local longitudinal and transverse directions at the abutment, based on the size and stress-strain response of expansion joint filler material [3]. With a compressive stress of 0.3625 ksi at 50 percent strain, the modulus of elasticity is 725 ksi.

Results from a modal analysis gave the 1st mode as a transverse response of the 2nd frame at a natural period of 2.45 seconds (Figure 24). Fourier Amplitude Spectra results show a definite spike at about 2.5 seconds at the same location. This indicates that the overall geometry, mass and stiffness of the model are realistic. Time-history analyses were conducted using modal analyses as well as direct time-stepping procedures and, so long as the damping provided was of the same form and magnitude, the results were virtually identical. Initially, modal time-history analyses were conducted with 2% and then 5% viscous damping. However, all of the analytical deformation results were much larger than measured, and in many cases more than twice the measured displacements. The final analysis results that have been included in this paper have 20 % damping applied to all modes, providing approximately the correct maximum deformations. It is probable that the additional damping is associated with soil response of the large diameter pile shafts and the abutments. Typically, for linear-elastic analysis or RC bridge structures 5% damping is used. For nonlinear analysis a more realistic number is thought to be 2%, with additional damping provided by the hysteretic behavior of the nonlinear elements. It is possible that the additional damping is related to the size of the earthquake motions, which are much smaller than expected from a maximum credible earthquake.

Up to this point in the project the bridge has been modeled with beam elements. However, the superstructure will be modeled with shell elements. Another possibility is that beam elements will continue to be used to model the superstructure in the global bridge modal and the beam element stiffness properties will be calibrated to results from a breakout shell element model of the superstructure from center-of-span to center-of-span, on either side of a typical bent. All of the behavior is still being modeled as linear-elastic, as the majority of the measured behavior is elastic. However, gapping elements will be provided locally at the interface between the abutment and bridge superstructure, so that no tension can be transferred across this joint. Also, damping elements will be provided to more correctly capture the local increased damping at the soil locations, allowing the damping for the remainder of the structure to be reduced to more realistic values.

The contents of this report were developed under Contract No. 1001-763 from the California Department of Conservation, California Geological Survey, Strong Motion Instrumentation Program. However, these contents do not necessarily represent the policy of that agency nor endorsement by the State Government.

References

[1] SAP2000, Version 8, (2002) User's Manual for computer program. CSI, Inc., Berkeley, California.

[2] Reese, L.C., (2000) User's Manual for computer program LPILE Plus, Version 4.0, ENSOFT, Inc., Austin, Texas.

[3] Sritharan, S., Preistley, M.J.N., Seible, F., (1997), "Seismic Design and Performance of Concrete Multi-Column Bents for Bridges", SSRP-97/03, Division of Structural Engineering, University of California at San Diego.

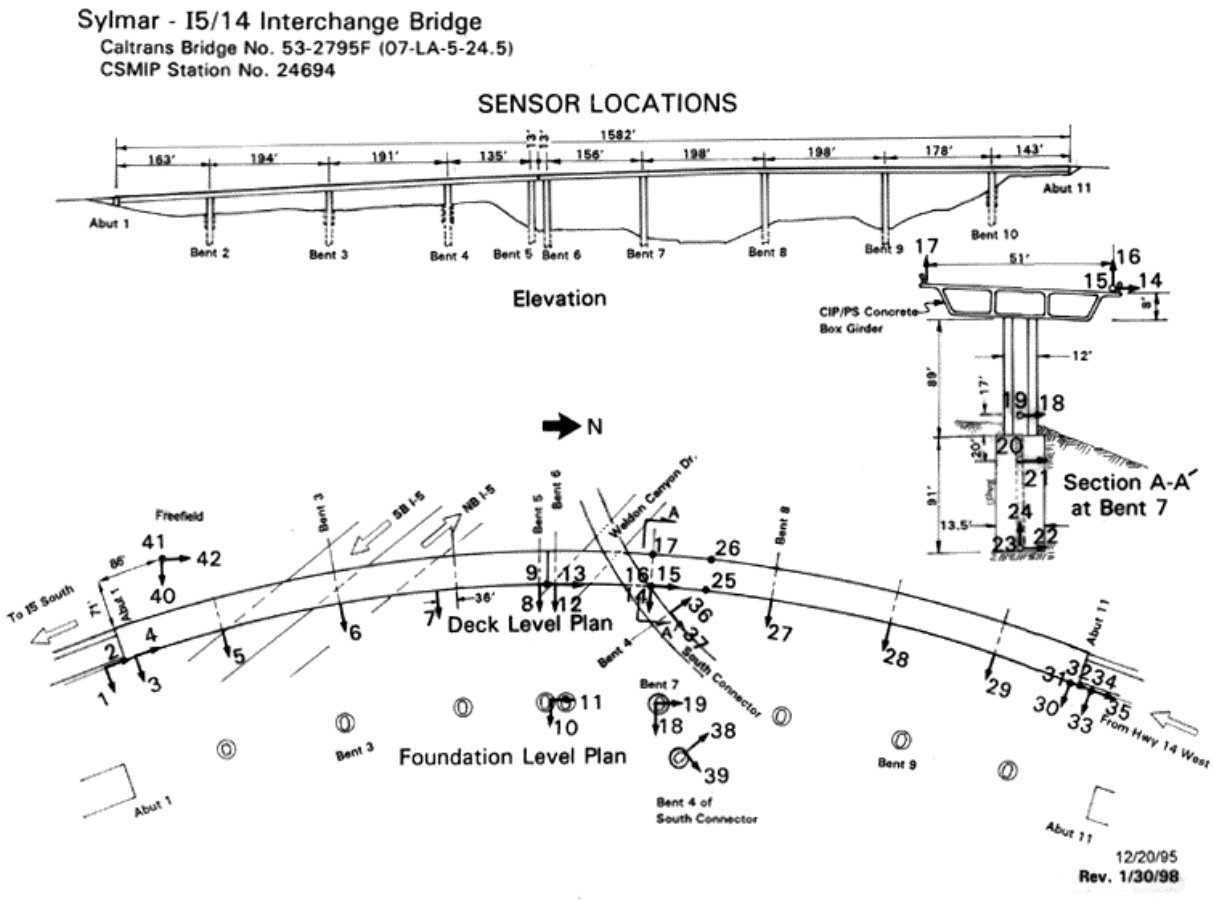

Figure 1. Sensor Locations and Overall Bridge Geometry

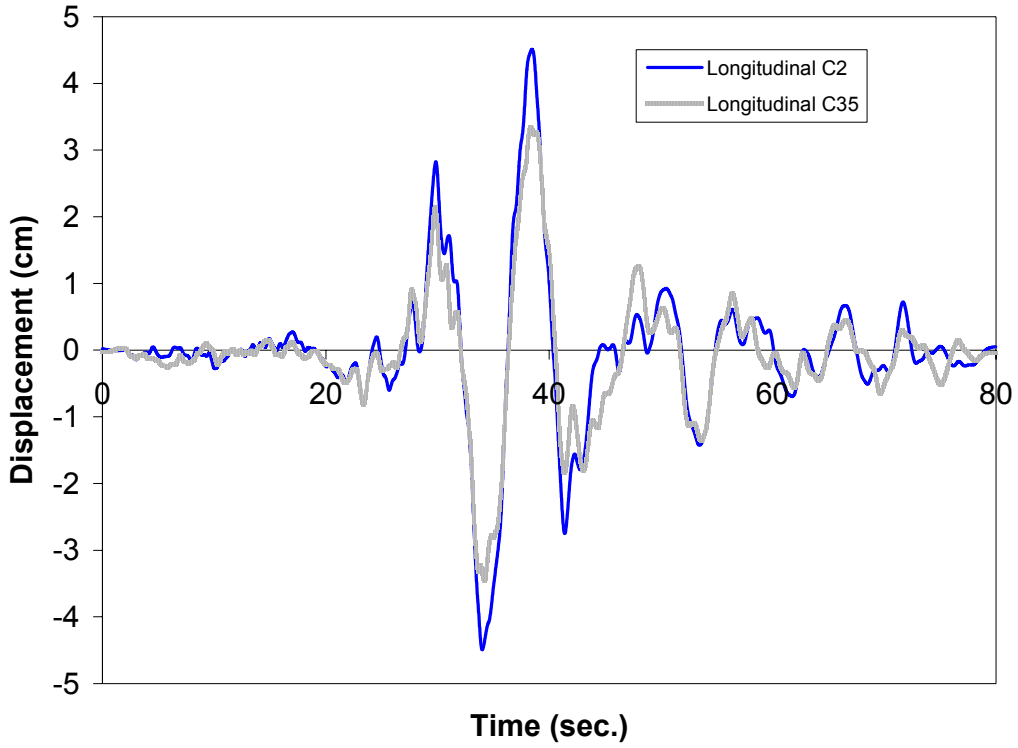

Figure 2. Local Longitudinal Response of Abutments 1 and 11

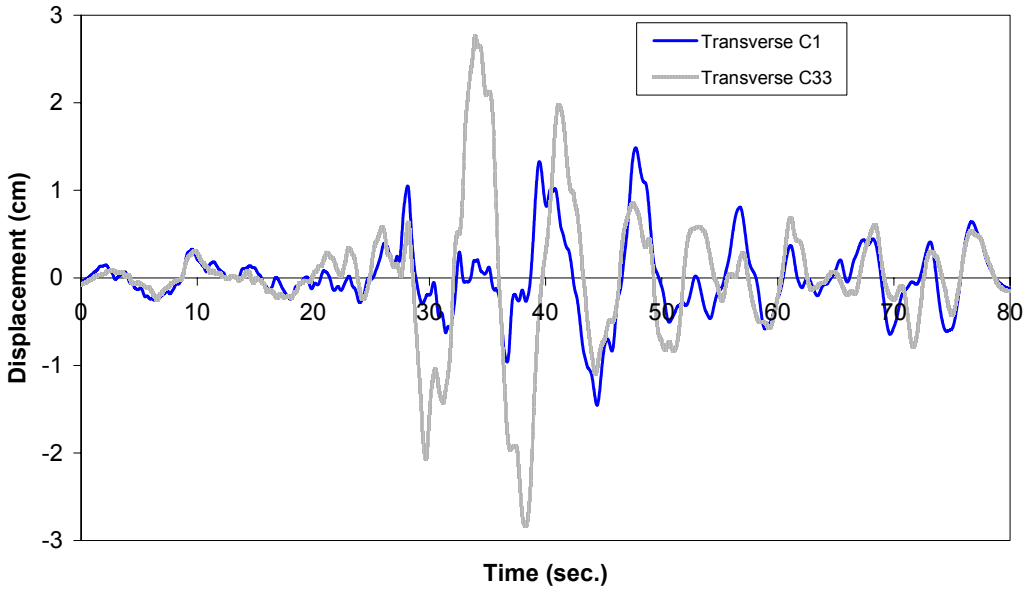

Figure 3. Local Transverse Response of Abutments 1 and 11

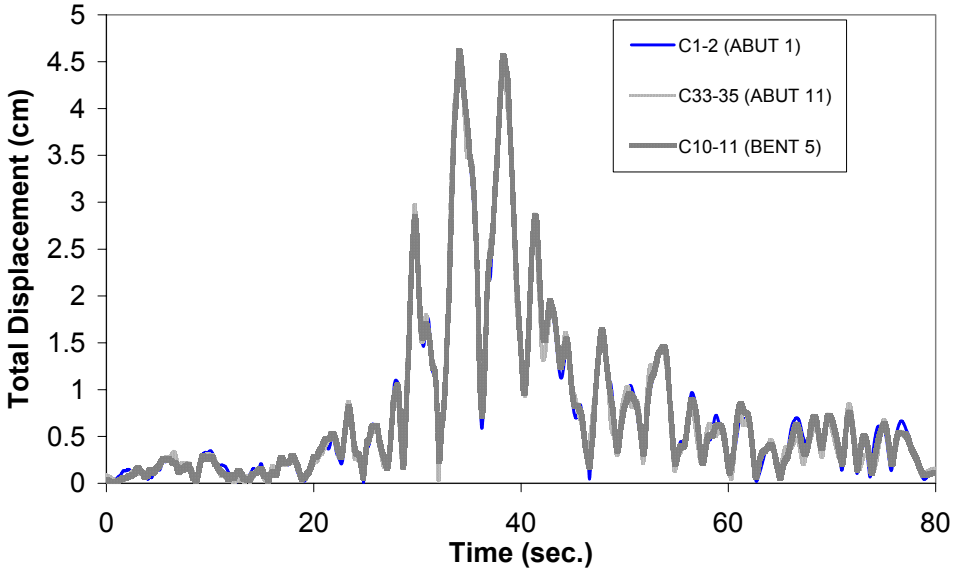

Figure 4. Total Response of Abutments 1 and 11 and Base of Bent 5 Column

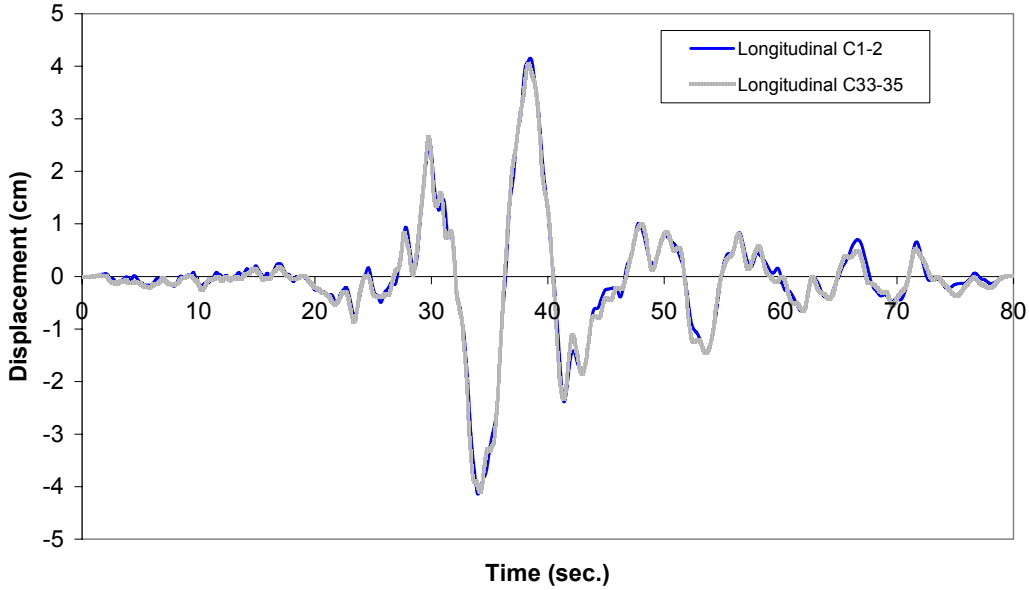

Figure 5. Global Longitudinal Response of Abutments 1 and 11

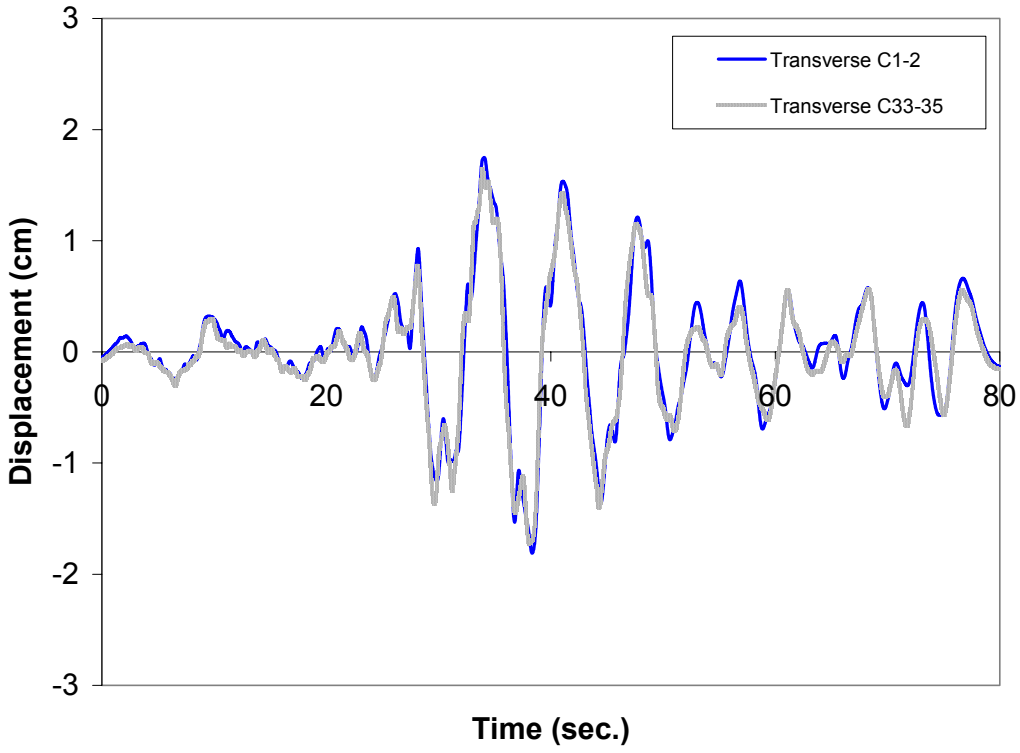

Figure 6. Global Transverse Response of Abutments 1 and 11

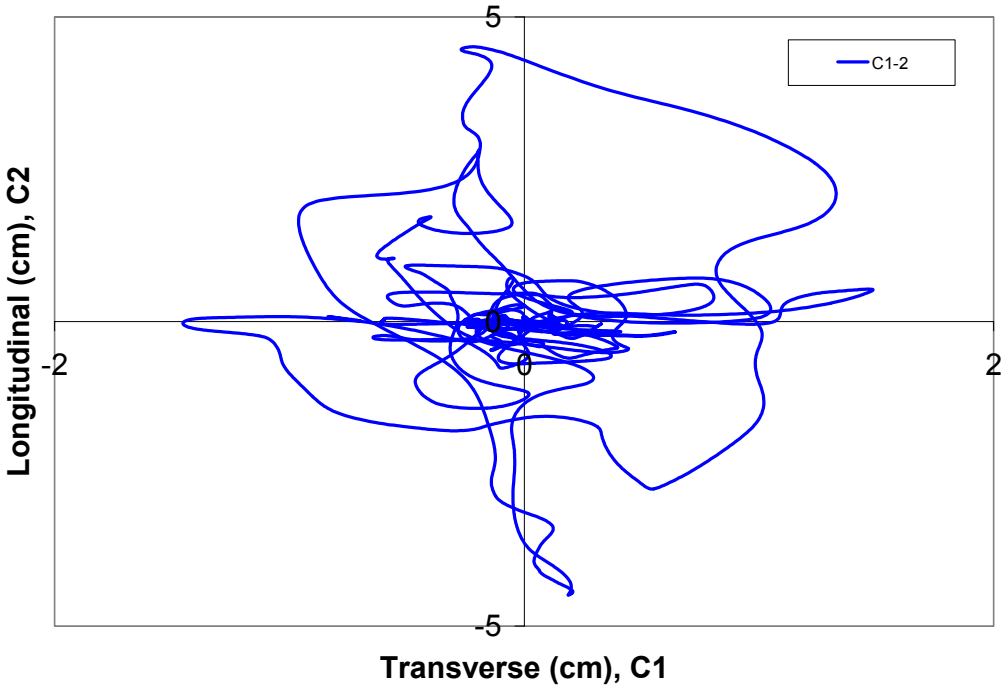

Figure 7. Local Transverse vs. Longitudinal Response at Abutment 1

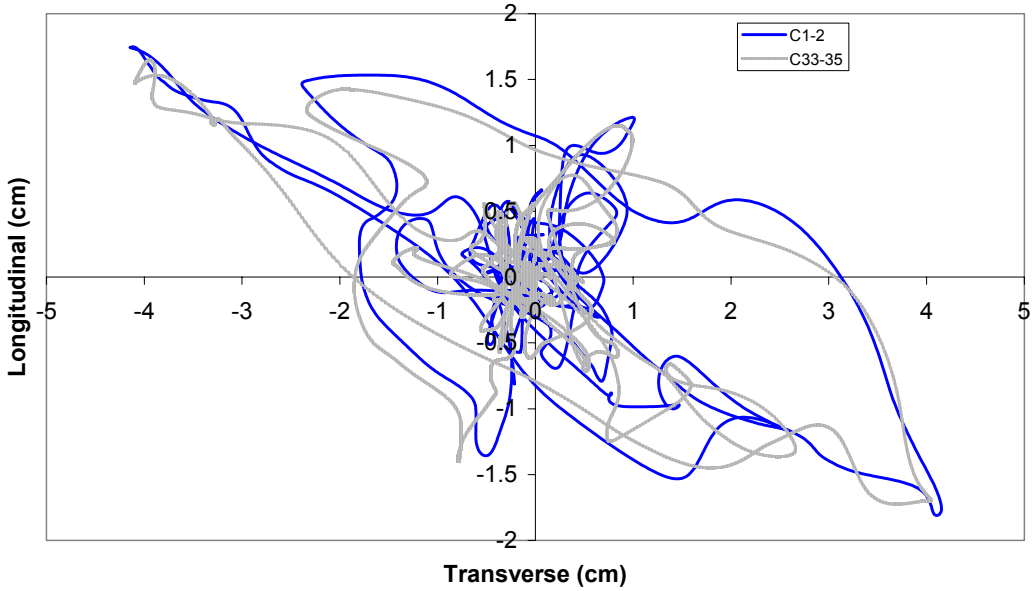

Figure 8. Global Transverse vs. Longitudinal Response at Abutments 1 and 11

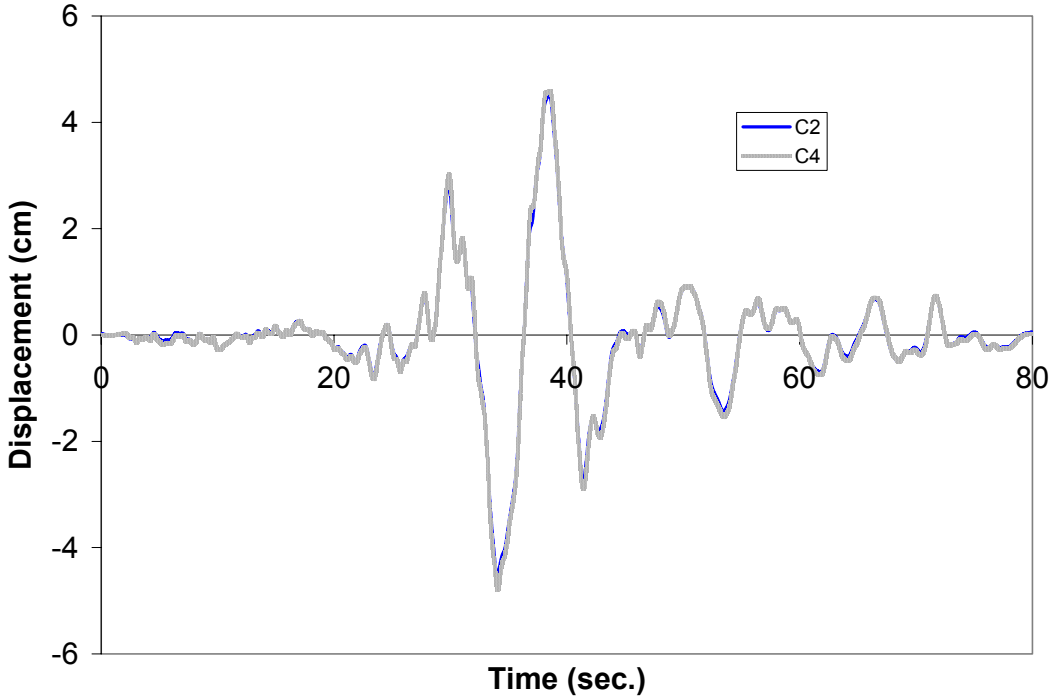

Figure 9. Local Longitudinal Response at Abutment 1

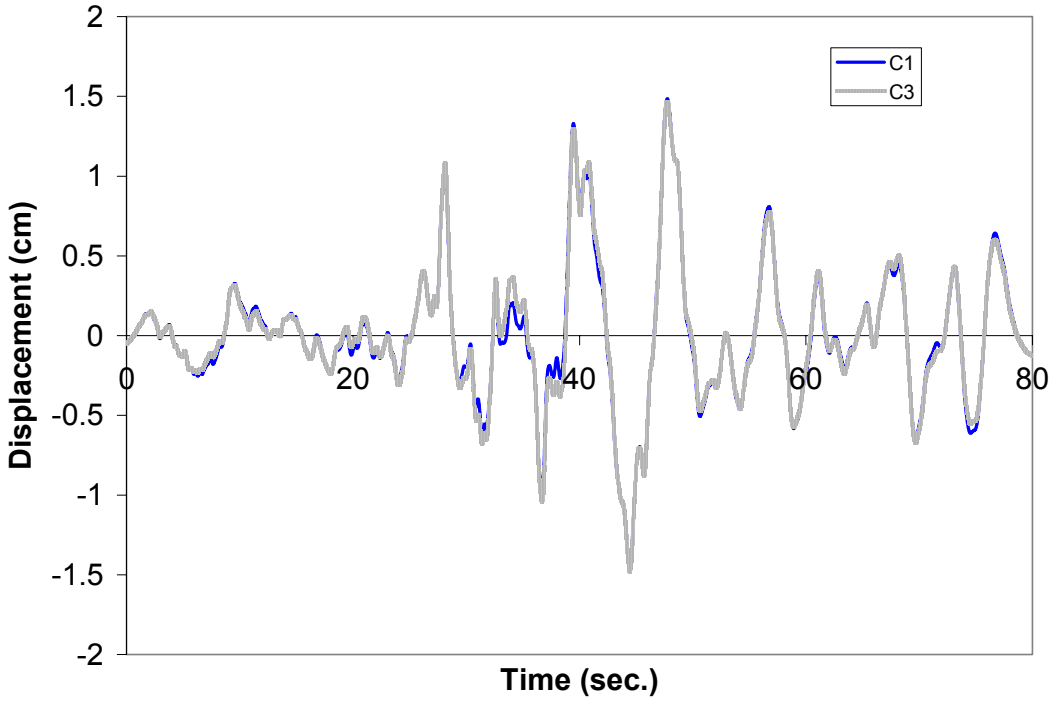

Figure 10. Local Transverse Response at Abutment 1

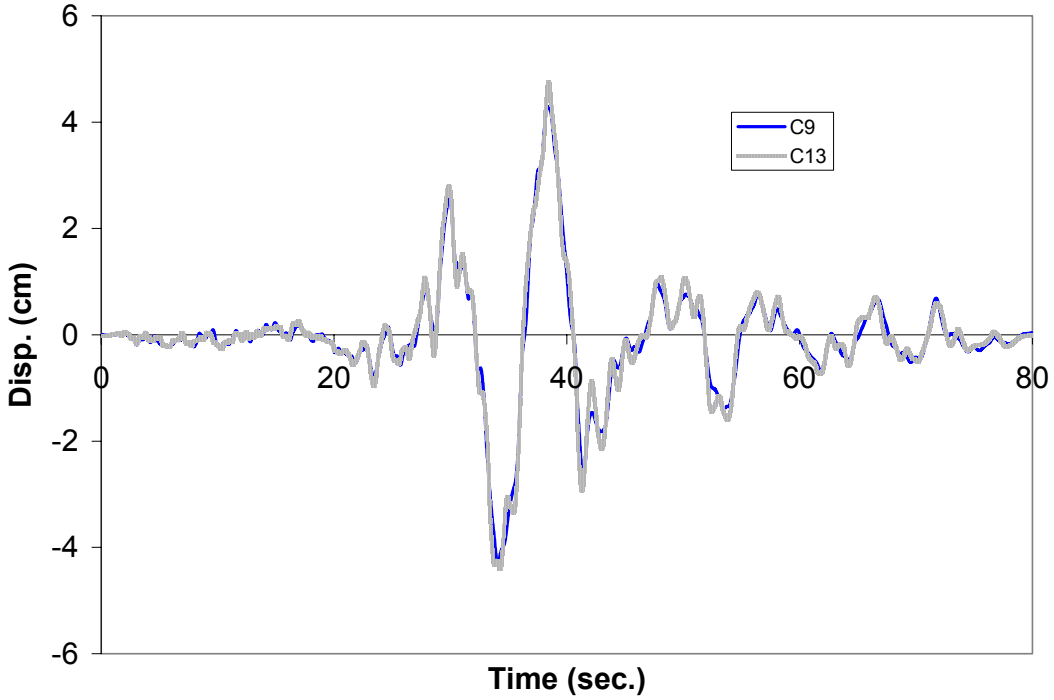

Figure 11. Local Longitudinal Response at Expansion Hinge Between Frames

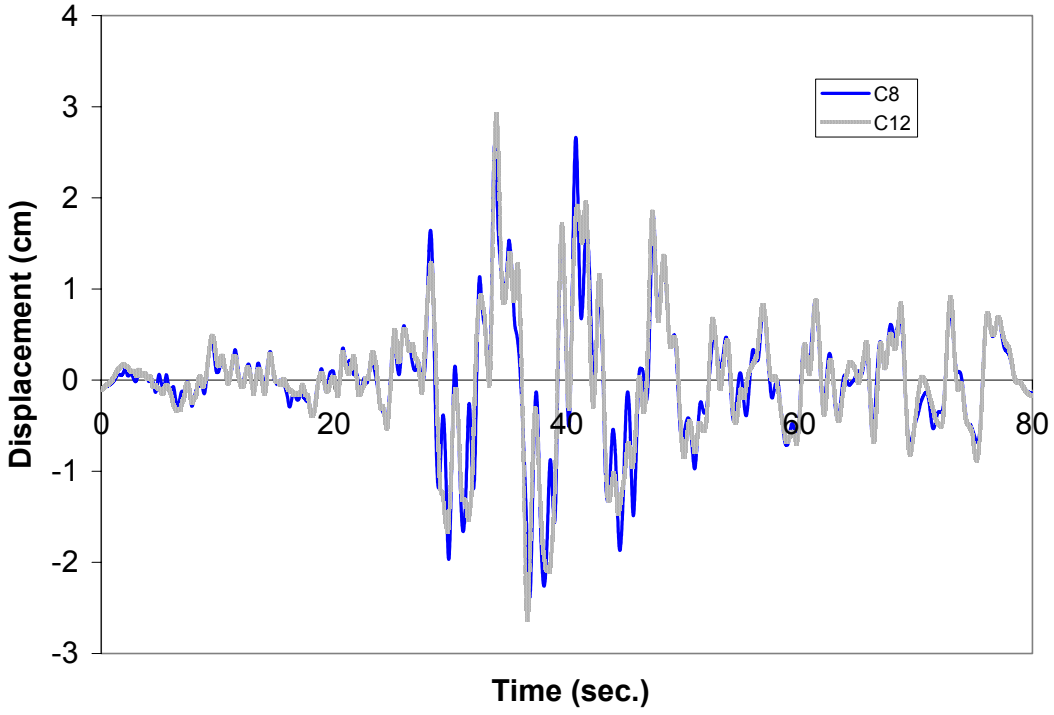

Figure 12. Local Transverse Response at Expansion Hinge Between Frames

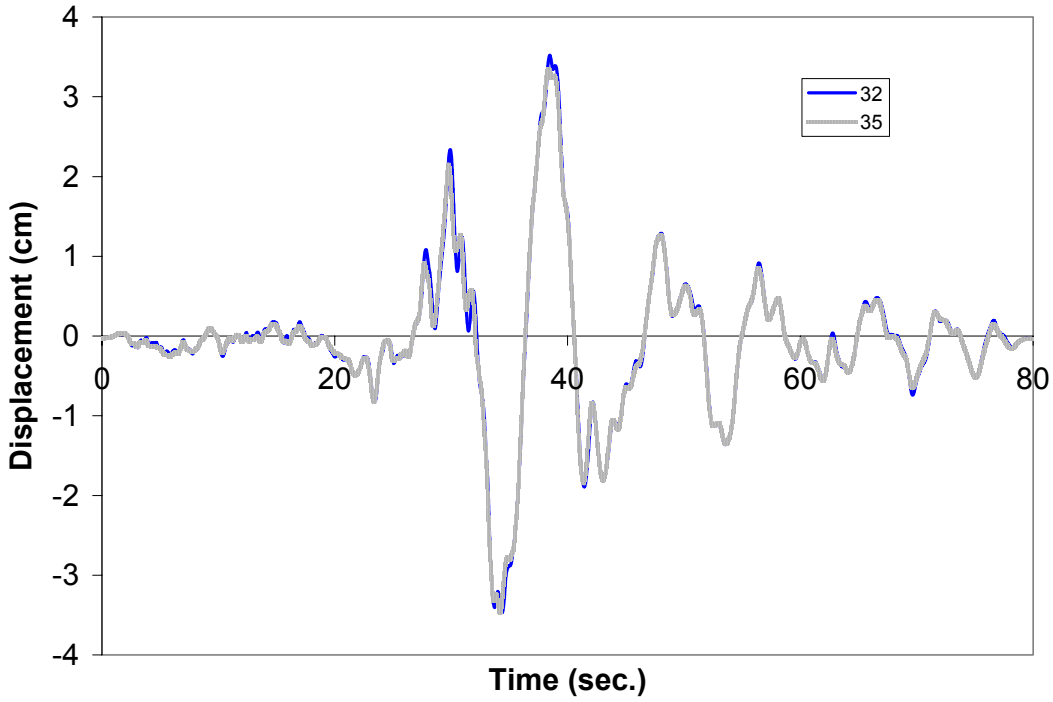

Figure 13. Local Longitudinal Response at Abutment 11

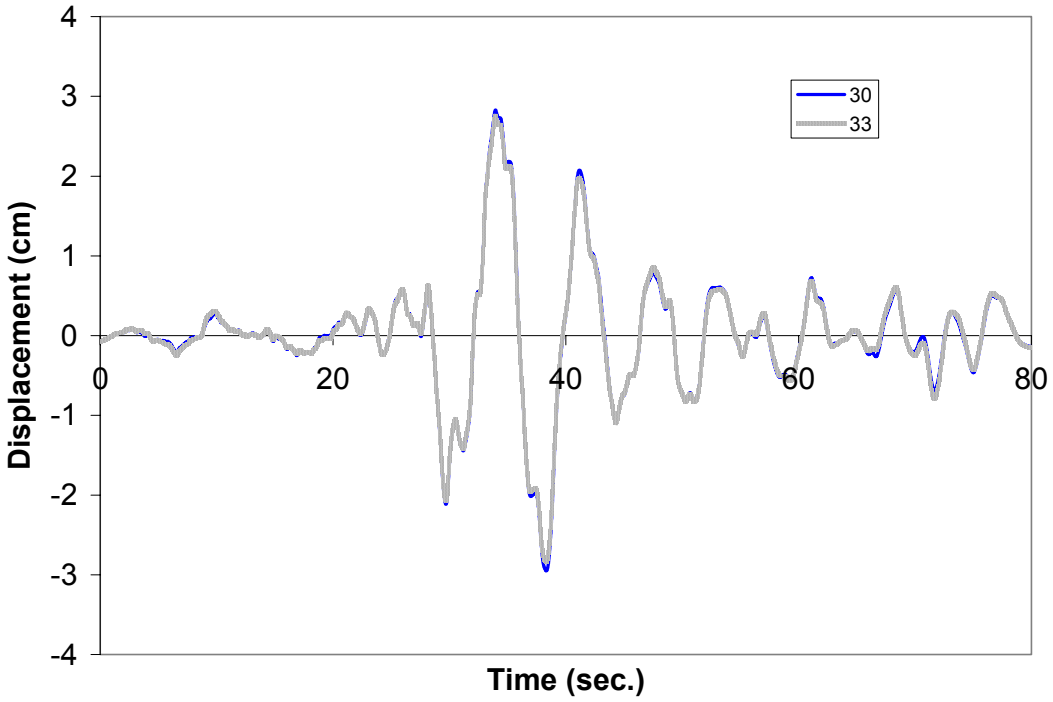

Figure 14. Local Transverse Response at Abutment 11

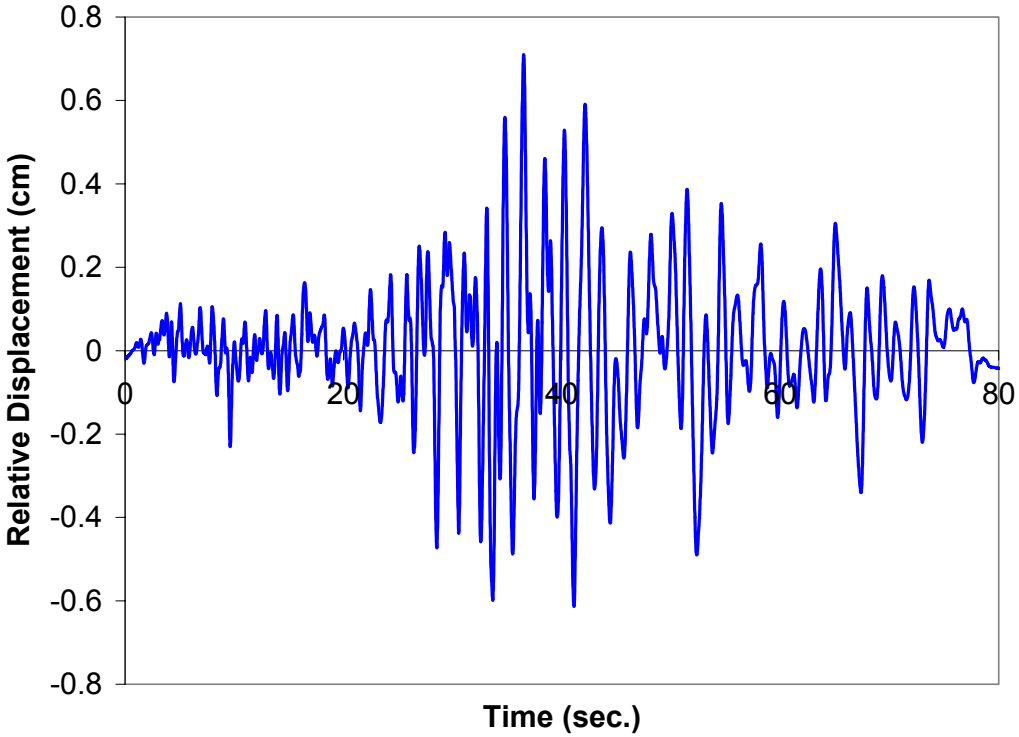

Figure 15. Relative Longitudinal Response at Expansion Hinge (local)

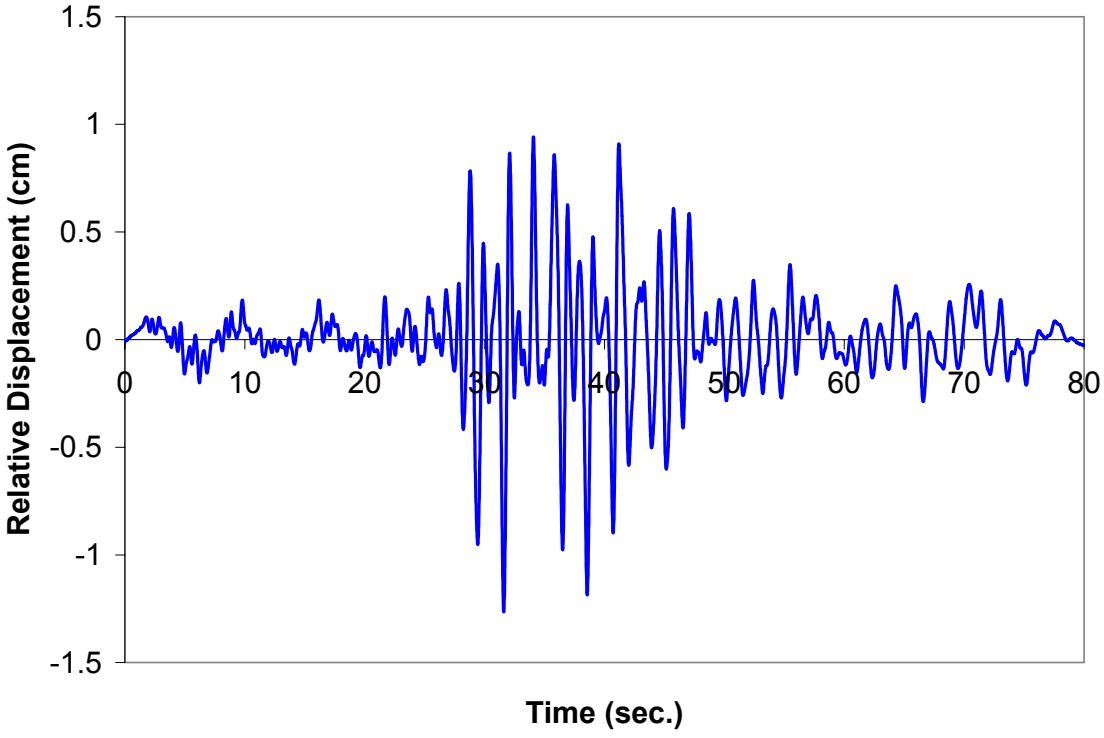

Figure 16. Relative Transverse Response at Expansion Hinge (local)

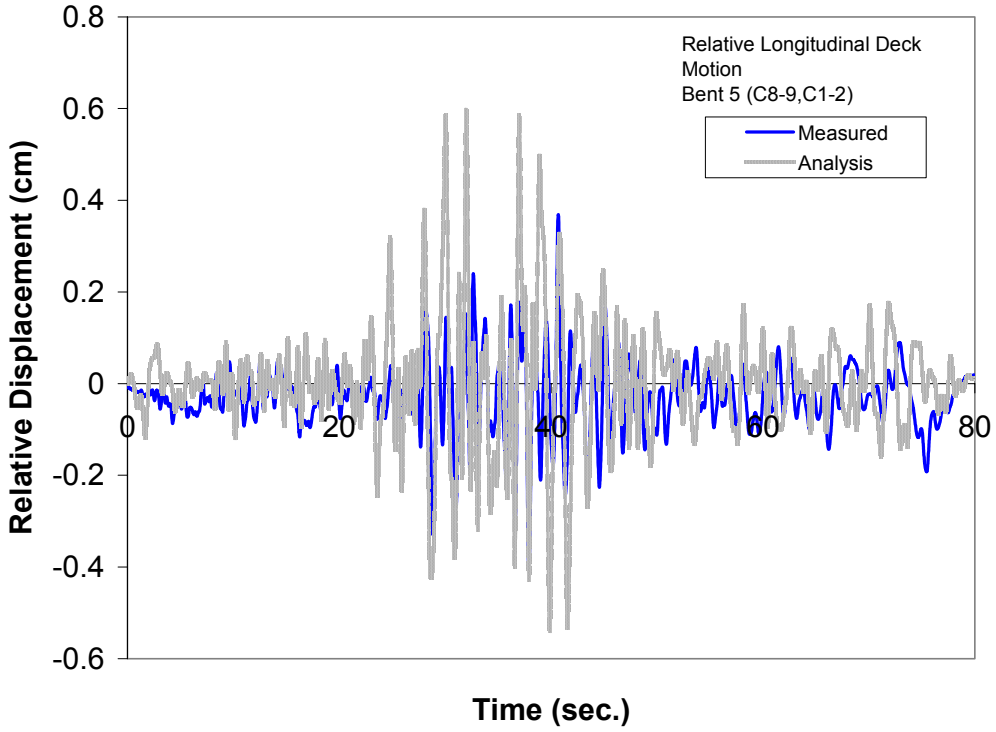

Figure 17. Relative Longitudinal Motion Between Deck at Bent 5 and Ground (analysis versus measured)

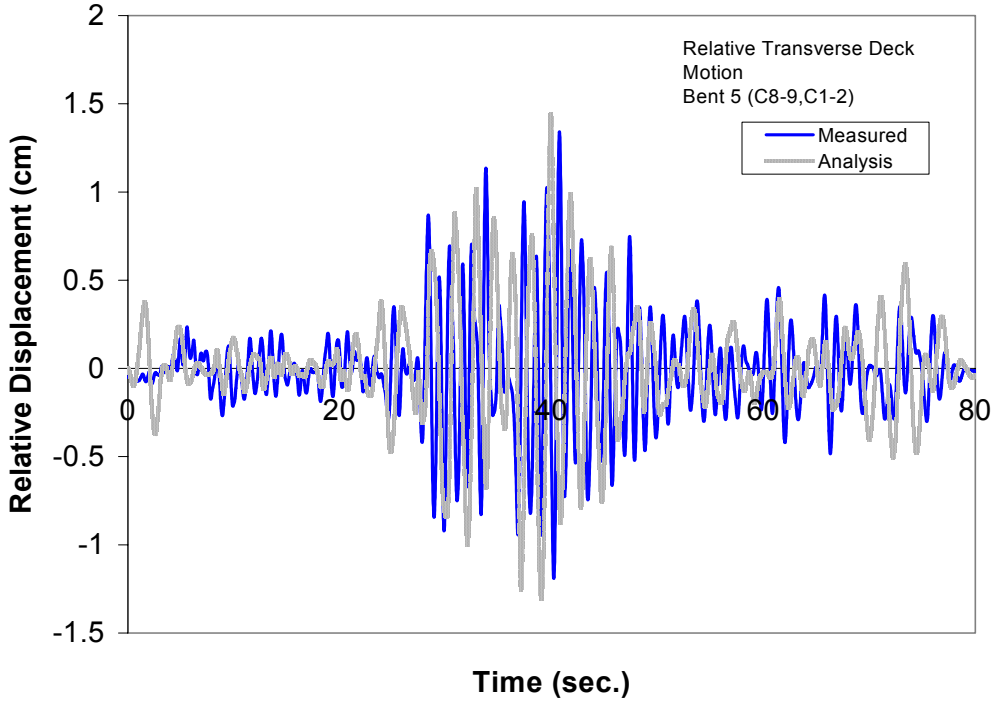

Figure 18. Relative Transverse Motion Between Deck at Bent 5 and Ground (analysis versus measured)

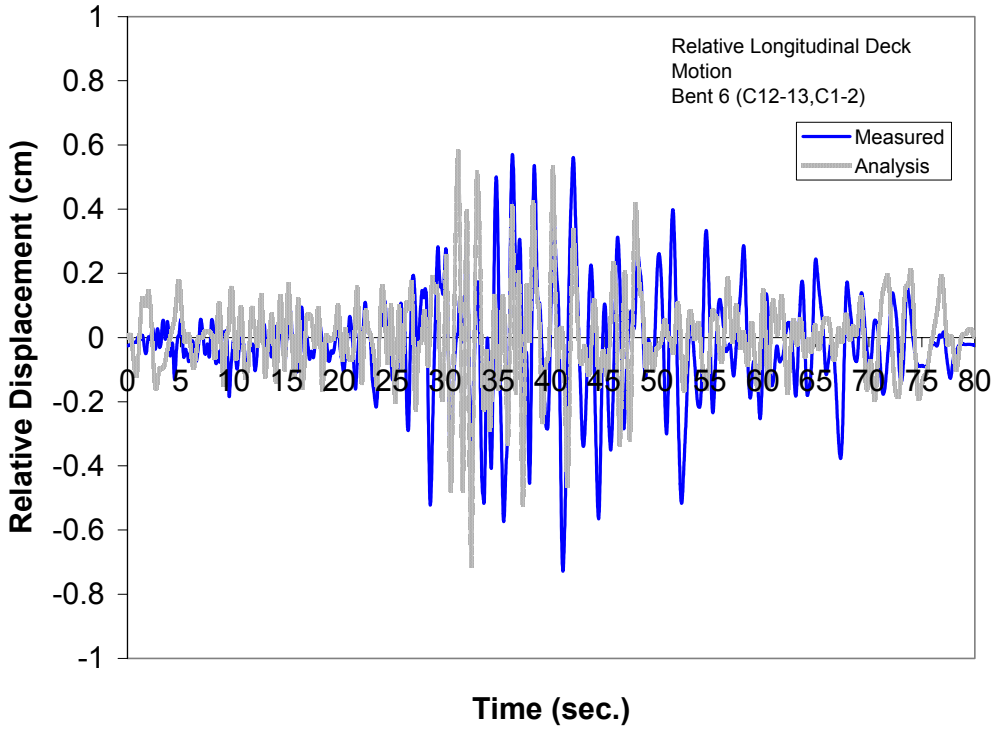

Figure 19. Relative Longitudinal Motion Between Deck at Bent 6 and Ground (analysis versus measured)

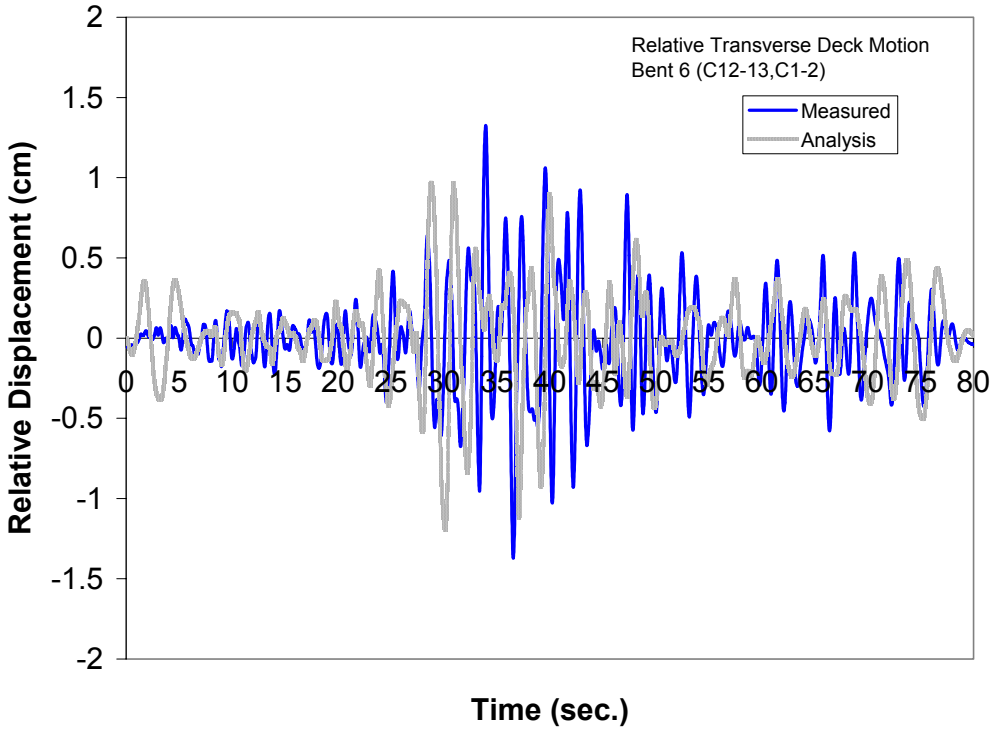

Figure 20. Relative Transverse Motion Between Deck at Bent 6 and Ground (analysis versus measured)

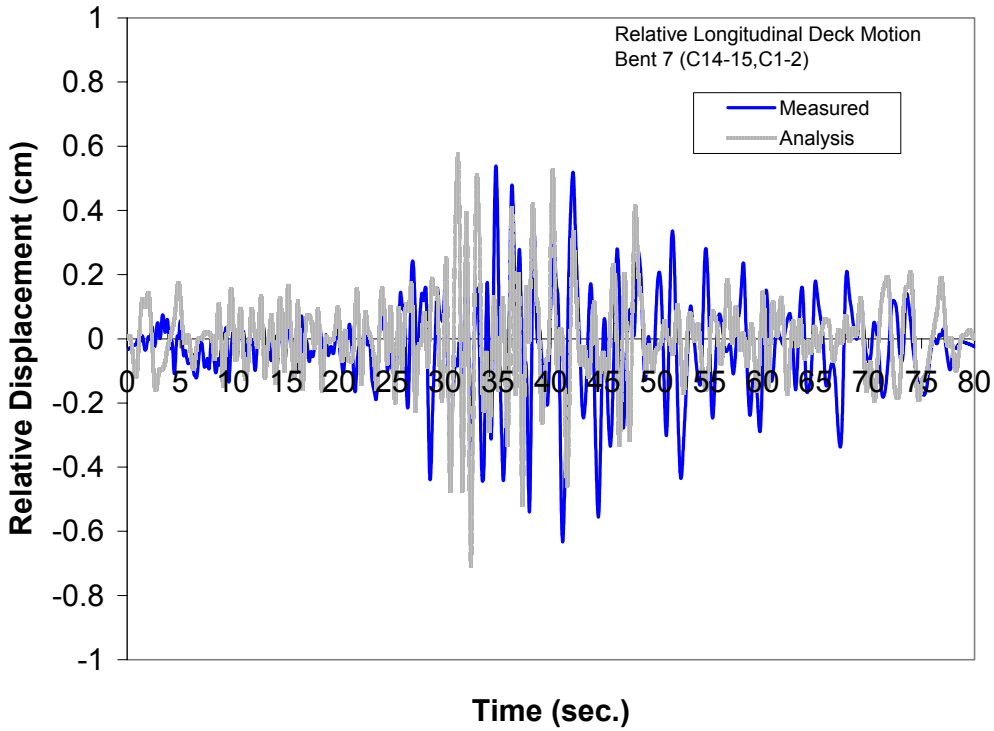

Figure 21. Relative Longitudinal Motion Between Deck at Bent 7 and Ground (analysis versus measured)

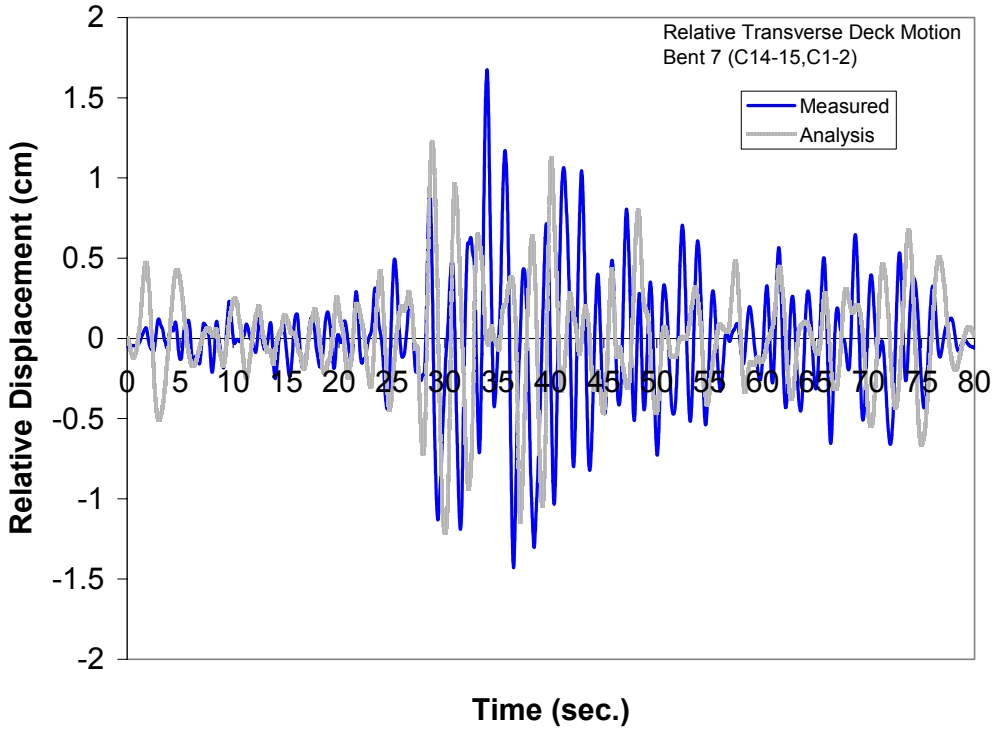

Figure 22. Relative Transverse Motion Between Deck at Bent 7 and Ground (analysis versus measured)

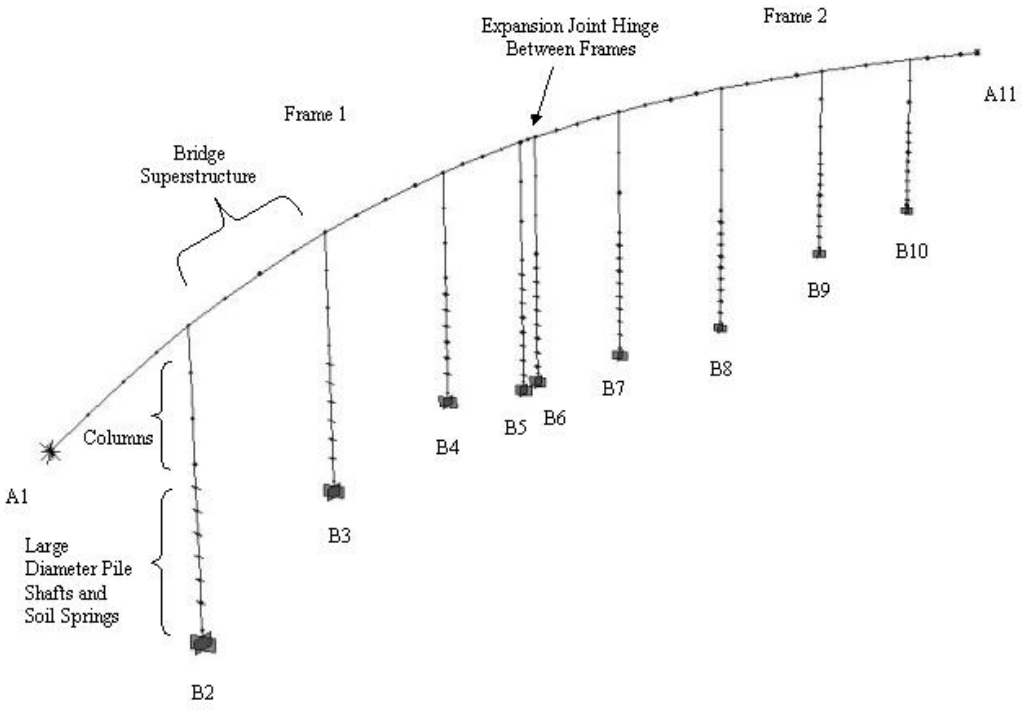

Figure 23. Global Bridge Model

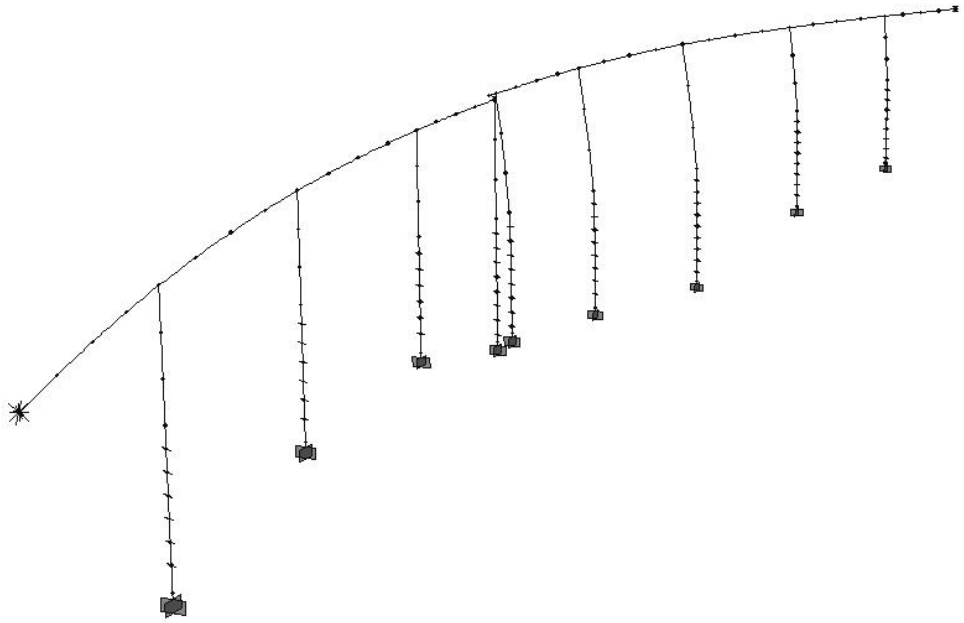

Figure 24. 1st Mode Response of Global Bridge Model